

Cite this: *RSC Adv.*, 2019, 9, 26109

# Preparation and characterization of cyanazine–hydroxypropyl-beta-cyclodextrin inclusion complex

Shuang Gao,<sup>a</sup> Chao Bie,<sup>a</sup> Qiuyu Ji,<sup>b</sup> Haiyang Ling,<sup>b</sup> Chunyan Li,<sup>c</sup> Ying Fu,<sup>a</sup> Lixia Zhao<sup>a</sup> and Fei Ye<sup>\*a</sup>

Due to its poor water solubility, the herbicide cyanazine is usually dissolved in organic reagents when used, which poses a great threat to the environment. Poor water solubility also causes limited herbicidal activity. In our study, the water solubility of cyanazine was increased by forming a cyanazine/hydroxypropyl beta-cyclodextrin (HP $\beta$ CD) inclusion complex. The formation of the inclusion complex was confirmed by FT-IR, XRD, SEM and other characterization methods. Phase solubility study showed that HP $\beta$ CD could improve the water solubility of cyanazine. Thermogravimetric analysis indicated that the thermal stability of cyanazine was improved by forming inclusion complex and the biological activity test showed that better herbicidal activity was obtained on the inclusion complex compared with the cyanazine. The results showed that the formation of inclusion complex could improve the application of cyanazine in agricultural production and reduce the risk to the environment.

Received 13th June 2019  
Accepted 14th August 2019

DOI: 10.1039/c9ra04448e

rsc.li/rsc-advances

## Introduction

Cyanazine (Fig. 1) is a selective systemic herbicide for crops such as corn, peas, and broad beans, which is used to control a variety of grass weeds and broadleaf weed.<sup>1</sup> Due to its poor water solubility, cyanazine is mostly dissolved in an organic solvent when used, which causes environmental pollution. It was urgent to find ways to improve the water solubility of cyanazine, and current research had proved that the formation of a HP $\beta$ CD inclusion complex was one of the effective approaches.<sup>2</sup>

HP $\beta$ CD (Fig. 2) is a hydroxyalkylated derivative of  $\beta$ CD, in which the hydrogen atom of the C-2, C-3 and C-6 hydroxyl group in the glucose residue is replaced by hydroxypropyl. HP $\beta$ CD was very important for supramolecular chemistry because it could form non-covalent complexes with a variety of host molecules and could be used as a model for studying weak interactions.<sup>3</sup> HP $\beta$ CD has a hydrophilic surface and a relatively hydrophobic cavity<sup>4</sup> wherein the lumen provided a suitable hydrophobic environment for the guest molecule.

Complexation based on cyclodextrin and cyclodextrin derivatives inclusion complex is widely used in food, agriculture and cosmetics.<sup>5</sup> Host–guest strategy has been well established in the literature, where HP $\beta$ CD is used as encapsulating agents

to complex with hydrophobic objects to increase their water solubility and bioavailability. For example, Wang *et al.* found that the amylose–HP $\beta$ CD inclusion complex was a promising technique to protect *p*-coumaric acid in foods during processing and storage while increasing its bioaccessibility.<sup>6</sup> Niclosamide–HP $\beta$ CD inclusion complex was prepared by freeze drying method. Compared with original niclosamide alone, *C*-max and *T*-max of niclosamide from HP $\beta$ CD inclusion complex were significantly improved and higher cytotoxicity at lower concentrations could be obtained.<sup>7</sup> Kfoury *et al.* reported an inclusion complex of cyclodextrins and caffeic acid, which was well-known as a natural beneficial to human body phenylpropanoid. Complexation with cyclodextrins could improve the poor aqueous solubility of caffeic acid while the antioxidant activity of caffeic acid in the inclusion complex was enhanced.<sup>8</sup> Supercritical antisolvent (SAS) process were performed to prepare inclusion complex of HP $\beta$ CD and simvastatin, which was a practically insoluble drug. Results showed that the aqueous solubility and the dissolution rate of drug were enhanced, as well as its bioavailability was improved.<sup>9</sup> Patel

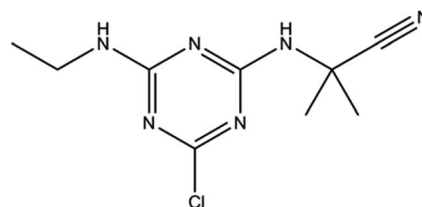


Fig. 1 Structure of cyanazine.

<sup>a</sup>Department of Applied Chemistry, College of Science, Northeast Agricultural University, Harbin, 150030, P. R. China. E-mail: yefei@neau.edu.cn

<sup>b</sup>School of Life Science, Northeast Agricultural University, Harbin, 150030, P. R. China

<sup>c</sup>College of Resources and Environment, Northeast Agricultural University, Harbin, 150030, P. R. China



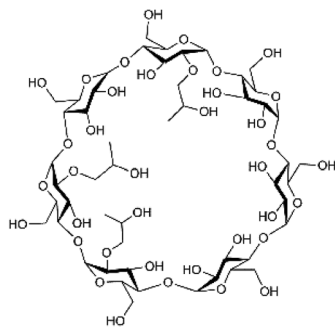


Fig. 2 The structure of HPβCD.

*et al.* indicated that tablets containing complexes of cyclodextrins and clonazepam showed significant improvement in the release profile of clonazepam, meaning that dissolution rate of clonazepam, which was a water-insoluble lipid-lowering drug, was improved by complexation.<sup>10</sup> Complexation with cyclodextrins and their derivatives was proved to be an effective approach to improve solubility, stability, and bioavailability of drug molecules. However, there was no report on HPβCD inclusion complex in which herbicide cyanazine acted as a guest molecule.

In this research, the inclusion complex of HPβCD and cyanazine was prepared through a co-precipitation method. Physicochemical properties of the inclusion complex were characterized by phase solubility diagram, TGA, FT-IR, XRD and SEM as well as the biological activity was tested to investigate the herbicidal activity of the inclusion complex.

## Experimental

### Materials

HPβCD (2-hydroxypropyl-β-cyclodextrin) was provided by Aladdin Reagent Co., Ltd. (Shanghai, China). Cyanazine was obtained from Dalian Meilun Biotech Co., Ltd. (Dalian, China). All other chemicals were obtained from Aladdin Reagent Co., Ltd. (Shanghai, China).

### Preparation of the inclusion complex

Inclusion complex of cyanazine with HPβCD was prepared in molar ratio of 1 : 1 *via* co-precipitation. Appropriate amount of HPβCD was dissolved in deionized water at room temperature to prepare a saturated aqueous solution, cyanazine was dissolved in acetone under stirring. The two solutions were mixed and continuously stirred at 55 °C for 3 hours. After being cooled at 0 °C for 12 hours, the suspension was filtered and the precipitate was washed with acetone to remove residual cyanazine. Then the precipitate was stored at 60 °C for 8 hours to remove solvent.

### Preparation of physical mixture

The physical mixture was prepared by mixing HPβCD and cyanazine in the same molar ratio as that used to prepare the

inclusion complex. Cyanazine and HPβCD were ground for 15 minutes to ensure homogeneous blend.

### Study of FT-IR

FT-IR spectra were recorded in KBr by an 8400S FT-IR spectrometer (Shimadzu, Kyoto, Japan) based on KBr disk technique. Baseline correction and spectral smoothing were applied. The FT-IR spectrometer was scanned in the range of 4000–400  $\text{cm}^{-1}$  at ambient temperature. The FT-IR spectrum of the inclusion complex was compared with those of pure cyanazine, HPβCD and physical mixture.

### Analysis of XRD

The powder sample was packaged from the top in an X-ray holder prior. The X-ray powder diffraction pattern was recorded on a Phillips X-ray diffractometer (Malvern Panalytical, Etten Leur, Netherlands) using Cu-K $\alpha$  radiation ( $\lambda = 1.5406 \text{ \AA}$ ), a voltage of 40 kV and a current of 30 mA. The scan rate used in the range of 5–90° was 2°  $\text{min}^{-1}$ .

### Study of SEM

The morphology of HPβCD and the inclusion complex was recorded using an SU-8010 environmental scanning electron microscope system (Hitachi Company, Tokyo, Japan). The sample was placed on a sample holder with an aluminum strip and sputter coated with thin gold layer under high vacuum using an acceleration voltage of 12.5 kV.

### Phase solubility study

Phase solubility study was performed according to Higuchi.<sup>11</sup> Excess cyanazine was added to a series of HPβCD aqueous solutions (0 to 10  $\text{mM L}^{-1}$ ). After being shaken at 25 °C for 48 hours, the above mixed solution was filtered using a 0.45  $\mu\text{m}$  cellulose filter. Finally, the amount of cyanazine dissolved in each filtrate was measured at 349 nm by a UV-visible dual beam spectrophotometer (UV-2550, Shimadzu, Suzhou, China).

The phase solubility diagram was plotted to indicate the apparent water solubility of cyanazine as a function of the HPβCD concentration.<sup>12,13</sup>

Formula (1) was used to calculate the associated constant value ( $K_f$ ):

$$K_f = \frac{\text{slope}}{S_0(1 - \text{slope})} \quad (1)$$

where  $S_0$  was the solubility of cyanazine in water, and slope represented the slope of the phase solubility diagram.

Formula (2) was used to calculate complexation efficiency (CE):

$$\text{CE} = S_0 \times K_f = \frac{[\text{HP}\beta\text{CD}/\text{cyanazine}]}{[\text{HP}\beta\text{CD}]} = \frac{\text{slope}}{1 - \text{slope}} \quad (2)$$

where  $[\text{HP}\beta\text{CD}/\text{cyanazine}]$  referred to the concentration of the inclusion complex and  $[\text{HP}\beta\text{CD}]$  was the concentration of free HPβCD. The phase solubility study could further analyze the



effect on the water solubility of cyanazine after the formation of the inclusion complex.<sup>14</sup>

To determine the stoichiometry and stability constant, the molar ratio of HP $\beta$ CD and cyanazine was continuously changed without altering the total molar concentration ( $c$  (cyanazine) +  $c$  (HP $\beta$ CD) =  $2 \times 10^{-5}$  mol L<sup>-1</sup>), and the difference in absorbances at 349 nm ( $\Delta A$ ) of the mixed solution and the cyanazine solution was recorded under the corresponding conditions. By plotting  $\Delta A$  versus  $r$ , the inclusion ratio could be calculated. The calculation of  $r$  value was shown in formula (3).

$$r = \frac{n(\text{cyanazine})}{n(\text{cyanazine}) + n(\text{HP}\beta\text{CD})} \quad (3)$$

### Study of TGA

Thermogravimetric analysis (TGA) of HP $\beta$ CD, cyanazine, physical mixture and the inclusion complex was performed by a thermogravimetric analyzer (Netzsch Company, Shanghai, China). A sample of about 3 mg was placed in a flat-bottomed aluminum pan and heated with the range from 50 °C to 800 °C by the rate of 10 °C min<sup>-1</sup> in dry nitrogen stream.

### Molecular modelling method

The 2D structure diagrams of HP $\beta$ CD and cyanazine were first drawn by ChemDraw, and the diagram was saved in cdx file format. Then, the above file was opened by Chem3D, and the software automatically outputted the 3D structure and save it as PDB file format. Subsequently, the molecules were optimized and the Gasteiger–Huckel charges were calculated. In Accelrys Discovery Studio 2.5 (Accelrys Inc., San Diego, CA, USA, 2005), the CDocker method was used for docking modelling.<sup>15,16</sup> Before docking, the cyclodextrin structure of the receptor was given a CHARMM force field and water was removed. After the HP $\beta$ CD preparation, the docking studies active site was defined, with a subset region of 13.0 Å from the center of the known ligand. The maximum hit was set to 100, and the rest use default parameters. The binding energy of the small molecule–receptor complex could be used as an evaluation index, which was the maximum negative expression of the most stable conformation.<sup>17</sup>

### Biological activity assay

*Echinochloa crusgalli* was chosen as the indicating weeds. After being soaked in water at 30 °C for 30 minutes, the seeds of the *Echinochloa crusgalli* were placed in a Petri dish in an incubator at 28 °C with a humidity of 78% for 12 hours. 15 seeds with the same shoot length were selected and sowed in a 7 × 7 cm plastic bowl. A total of 20 cups of *Echinochloa crusgalli* were planted. After 15 days of growth under indoor lighting, the above 20 cups of *Echinochloa crusgalli* were equally divided into 4 groups of 5 cups each. Cyanazine (0.045 mmol m<sup>-2</sup>), physical mixture (0.045 mmol m<sup>-2</sup>), the inclusion complex (0.045 mmol m<sup>-2</sup>) and water were sprayed on the leaves of each group. The growth index of *Echinochloa crusgalli* seedlings including root length, plant height and fresh weight were

determined after 10 days. Each treatment was replicated thrice.

Chlorophyll content was measured by spectrophotometry.<sup>18</sup> The leaves of valerian were washed and shredded. 0.1 g of leaves were weighed by an analytical balance (AU120 Shimadzu, Japan) and soaked in mixed solvent ( $V_{\text{acetone}} : V_{\text{ethanol}} : V_{\text{water}} = 16 : 19 : 5$ ). 10 mL of mixed solution was immersed in the dark for 14 hours until the leaves turned white. After filtration, the volume was determined. The absorbance was measured at 645 nm and 663 nm. The chlorophyll content was calculated according to the following formula (4) and (5):

$$C_a = (12.72A_{663} - 2.59A_{645})V/W \quad (4)$$

$$C_b = (22.88A_{645} - 4.68A_{663})V/W \quad (5)$$

where  $C_a$  was the content of chlorophyll a (mg);  $C_b$  was the content of chlorophyll b (mg);  $A_{645}$  and  $A_{663}$  represented optical densities at 645 nm and 663 nm wavelengths, respectively;  $V$  was the constant volume (mL) and  $W$  was the nominal sample volume (g). The experiment was carried out with three replicates.

## Results and discussions

### FT-IR analysis

FT-IR spectroscopy was considered as a useful technology to provide information about functional groups of components. The shape, position and strength of the absorption bands of the different samples were changed and were recorded in Fig. 3.

Obvious peaks at 3380 cm<sup>-1</sup>, 2903 cm<sup>-1</sup> and 1029 cm<sup>-1</sup> were obtained in the FT-IR spectrum of HP $\beta$ CD. The FT-IR spectrum of cyanazine showed a stretching vibration peak of –NH at 3231 cm<sup>-1</sup>, a peak at 2338 cm<sup>-1</sup>, and a sharp medium-intensity peak at 1528 cm<sup>-1</sup>. The FT-IR spectrum of the physical mixture was a simple superposition of cyanazine and HP $\beta$ CD. The FT-IR spectrum of the inclusion complex was

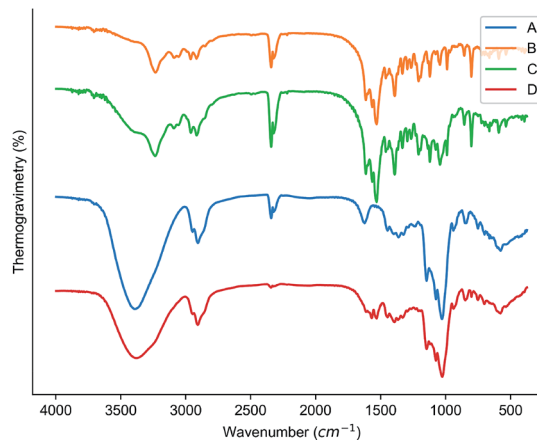


Fig. 3 Results of FT-IR: (A) HP $\beta$ CD; (B) cyanazine; (C) physical mixture; and (D) the inclusion complex.



different from the pure cyanazine, HP $\beta$ CD and physical mixture. Peaks in FT-IR spectrum of cyanazine at 2338  $\text{cm}^{-1}$ , 1528  $\text{cm}^{-1}$ , and 800  $\text{cm}^{-1}$  were not found in FT-IR spectrum of the inclusion complex, while the medium-intensity peak at 3231  $\text{cm}^{-1}$  completely disappeared. The peak in FT-IR spectrum of HP $\beta$ CD at 3383  $\text{cm}^{-1}$  became wider in the FT-IR spectrum of the inclusion complex. The reason might be that the vibration of the cyanazine molecule was limited when the cyanazine molecule was encapsulated into the HP $\beta$ CD cavity. The strength of the interaction between the host and guest molecules, such as hydrophobic interaction, dipole interaction, van der Waals force, *etc.*, played a crucial role in the formation of the inclusion complex. The FT-IR study could visually compare the difference in peak positions of cyanazine, HP $\beta$ CD, physical mixture and the inclusion complex, which was one of the favorable evidences for formation of the inclusion complex.<sup>19,20</sup>

### Analysis of XRD

The results of XRD analysis could be used as one of the strongest evidences for the formation of the inclusion complex.<sup>21,22</sup> The results of the XRD analysis were shown in Fig. 4. It was observed that there is no particularly obvious peak in the XRD spectrum of HP $\beta$ CD, which indicated that HP $\beta$ CD was amorphous; the XRD spectrum of the cyanazine had obvious sharp peaks at 12.22°, 16.92° and 19.13°. The cyanazine was in a crystalline state; the peak position observed in the XRD spectrum of the physical mixture was very similar to the cyanazine, but the intensity of the peak was lower than that of the herbicide; the XRD spectrum of the inclusion complex and the XRD spectrum of HP $\beta$ CD were similar, indicating that the inclusion complex lacks crystallinity. According to Williams *et al.*<sup>23</sup> lack of crystallinity is one of the favorable evidences for the formation of inclusion complexes. It could be speculated that the inclusion complex has formed, cyanazine molecules dispersed in the flexible cavity of the HP $\beta$ CD in an amorphous state, which was consistent with the existing research results.<sup>24,25</sup>

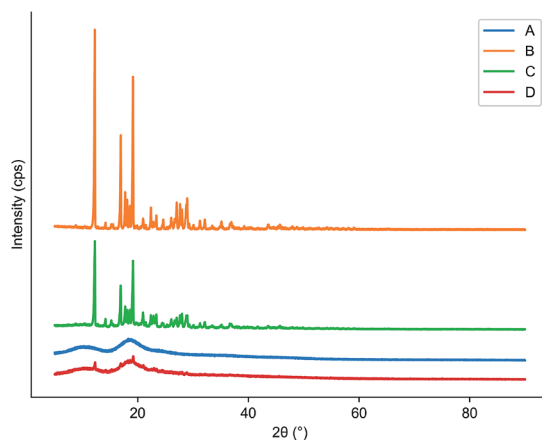


Fig. 4 Results of XRD: (A) HP $\beta$ CD; (B) cyanazine; (C) physical mixture; and (D) the inclusion complex.

### Results of SEM

SEM could provide us with an intuitive image to analyze whether the inclusion complex had been successfully formed by comparing the image differences between HP $\beta$ CD and the inclusion complex.<sup>26</sup> Fig. 5 was a scanning electron micrograph of HP $\beta$ CD and inclusion complex. SEM could be used to describe changes in crystal state and spatial structure. HP $\beta$ CD was spherical and porous, and the cyanazine presented as a long strip, while the cyanazine/HP $\beta$ -CD physical mixture was a simple mixed accumulation of HP $\beta$ -CD and cyanazine. After the inclusion complex was formed, the crystallinity of cyanazine molecules entering the HP $\beta$ CD cavity may decrease or even disappear, and at the same time changes will occur in the crystal state and spatial structure. SEM image of HP $\beta$ CD was spherical and porous. In the SEM image of the inclusion complex, irregular and various bulk crystal structures with loose connections could be observed on its surface. These morphological changes indicate that inclusion complex had been formed, and the interaction between cyanazine and HP $\beta$ CD molecules was the main reason for the significant changes in the morphology of HP $\beta$ CD molecules.<sup>27</sup>

### Phase solubility study

Fig. 6 was the dissolution change of cyanazine in HP $\beta$ CD solution with different concentrations. According to the research of Higuchi *et al.*, it could be known that the solubility curve belongs to  $A_L$  type, and it could be concluded that the water solubility of cyanazine also shown a linear increasing trend with the increase of HP $\beta$ CD concentration. According to formula,  $K_f$  value could be calculated to be  $2300 \pm 230 \text{ M}^{-1}$ , which indicated that cyanazine molecules could be closely combined with HP $\beta$ CD. The CE value could be calculated to be  $0.90 \pm 0.08$ , indicating that HP $\beta$ CD had the potential to dissolve cyanazine molecules. The above research results showed that HP $\beta$ CD could significantly improve the water solubility of cyanazine and had certain research value.

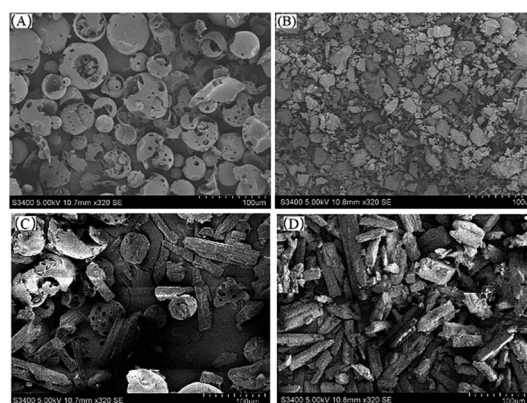


Fig. 5 SEM image of (A) HP $\beta$ CD, (B) the inclusion complex, (C) physical mixture and (D) cyanazine.



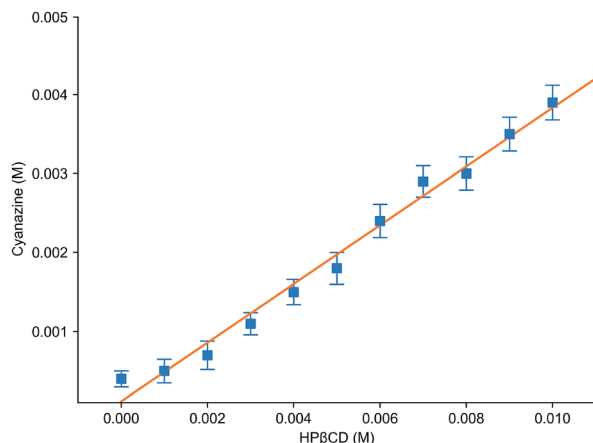


Fig. 6 Phase solubility study of the inclusion complex.

### Study of inclusion ratio

The inclusion ratio test results of inclusion complex were shown in Fig. 7.  $r$  represented the molar ratio of cyanazine in the mixed solution of cyanazine and HP $\beta$ CD, and  $\Delta A$  represented the difference between the absorbance of cyanazine in the mixed solution and the UV absorbance of cyanazine with the same concentration when HP $\beta$ CD was not added. It could be clearly seen from the Fig. 7 that when  $r = 0.5$ , the value of  $\Delta A$  was the largest, HP $\beta$ CD had the greatest influence on the absorbance of cyanazine, and proving that the inclusion complex was formed according to the molar ratio of 1 : 1.

### Study of TGA

TGA could help us check the thermal stability of pure cyanazine, HP $\beta$ CD, physical mixture and the inclusion complex. Fig. 8 showed that the thermal weight loss process of HP $\beta$ CD was carried out in two stages, the first stage was from 200 °C to 250 °C, which was the process of HP $\beta$ CD losing crystal water; the second stage was from 250 °C to 400 °C, which was the thermal decomposition process of HP $\beta$ CD. At 50 °C, the physical mixture began to lose weight, and a large weightlessness

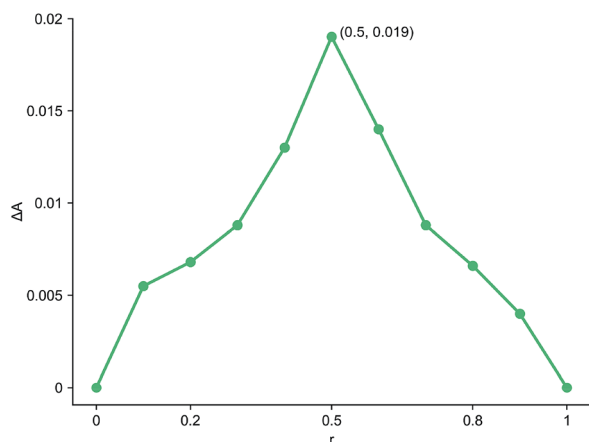


Fig. 7 Study of inclusion ratio.

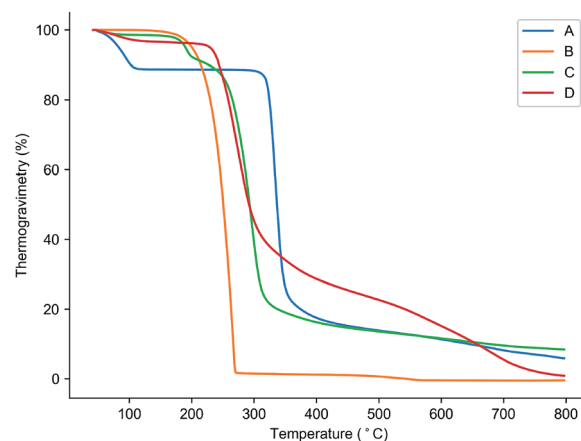


Fig. 8 Results of TGA: (A) physical mixture; (B) cyanazine; (C) HP $\beta$ CD; and (D) the inclusion complex.

step appeared at 302 °C, after this process, the physical mixture was almost completely decomposed. The inclusion complex began to lose weight at 231 °C, and the rate of weight loss was relatively slow. It was almost completely decomposed at 700 °C. The above results indicated that the inclusion complex had the strongest thermal stability, which was related to the cavity matching between cyanazine molecule and HP $\beta$ CD.

### Results of molecular modelling

Molecular modelling was performed to study the complexation between host molecules and guest molecules.<sup>28,29</sup> The molecular model in Fig. 9 was the lowest energy model obtained by molecular modelling. The results showed that small molecule cyanazine and large molecule cyclodextrin were effectively combined. In addition, the host and the guest form multiple hydrogen bonds to maintain the supramolecular structure.

### Results of biological activity assay

As shown in Fig. 10, it was the effect of spraying cyanazine, the physical mixture and inclusion complex on the growth index of *Echinochloa crusgalli*. The experimental results showed that the

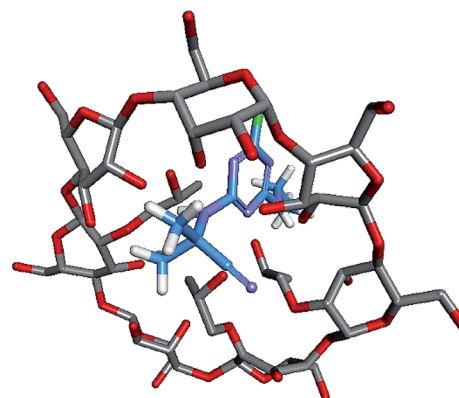


Fig. 9 The docking modelling of cyanazine and HP $\beta$ CD.



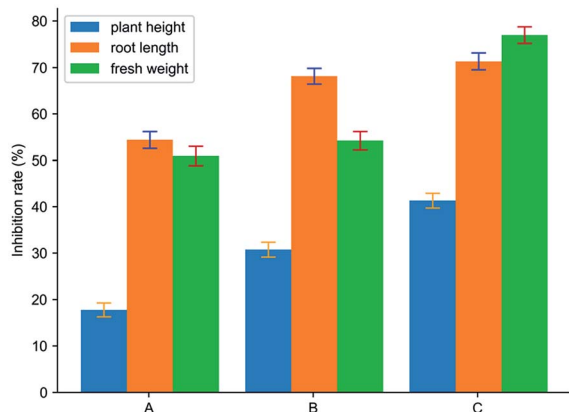


Fig. 10 The result of biological activity assay: (A) cyanazine; (B) physical mixture; and (C) the inclusion complex.

average root length of the cyanazine-dried *Echinochloa crusgalli* was  $4.77 \pm 0.11$  cm, the average plant height was  $15.08 \pm 0.14$  cm, the average fresh weight was  $0.060 \pm 0.001$  g; the average root length of the *Echinochloa crusgalli* sprayed with the physical mixture was  $3.33 \pm 0.11$  cm, the average plant height was  $12.70 \pm 0.12$  cm, the average fresh weight was  $0.056 \pm 0.002$  g. The above research results indicated that both the physical mixture and the inclusion complex had certain herbicidal activity, but the inclusion complex had the strongest herbicidal activity, which was related to the enhanced water solubility of the cyanazine.

Fig. 11 showed the effect of spraying water, HP $\beta$ CD, cyanazine, the physical mixture and inclusion complex on the contents of two chlorophyll in *Echinochloa crusgalli*. The experimental results showed that the contents of chlorophyll in *Echinochloa crusgalli* sprayed with water and HP $\beta$ CD did not have significant difference, indicating that HP $\beta$ CD did not have herbicidal activity. Chlorophyll content in *Echinochloa crusgalli* sprayed with cyanazine decreased. Chlorophyll content in *Echinochloa crusgalli* sprayed with physical mixture and inclusion complex decreased obviously, indicating that both had certain herbicidal activity. The content of chlorophyll in the

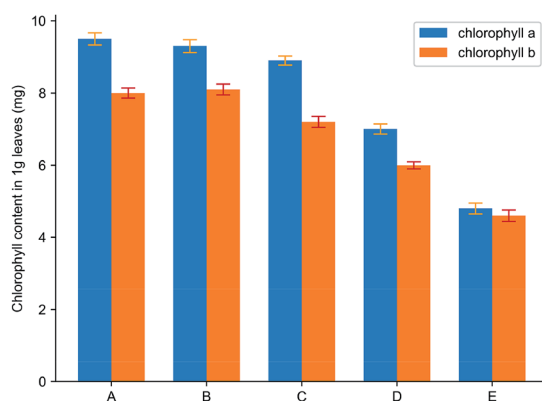


Fig. 11 The result of chlorophyll content: (A) water; (B) HP $\beta$ CD; (C) cyanazine; (D) physical mixture and (E) the inclusion complex.

alfalfa treated by the inclusion complex was the lowest, indicating that the herbicidal activity of the inclusion complex was stronger, which may be related to HP $\beta$ CD's ability to enhance the water solubility of cyanazine, resulting in an increase in the concentration of the cyanazine in the solution, so that the herbicidal activity was enhanced.

## Conclusions

Cyanazine is hardly soluble in water and needs to be dissolved in organic solvent, which causes environmental pollution during use. The inclusion complex with cyclodextrin derivative can improve its water solubility and thermal stability. The experimental results showed that the inclusion complex formed by cyanazine and HP $\beta$ CD could change the morphology of HP $\beta$ CD. By the phase solubility study, it was found that the water solubility and thermal stability of cyanazine were enhanced after forming the inclusion complex, these two properties are positively correlated with the concentration of HP $\beta$ CD. Bioassay results showed that the inclusion complex retained the activity of cyanazine and enhanced the herbicidal effect. The above research results showed that the formation of the inclusion complex could better play the role of cyanazine in agricultural production and was more environmentally friendly.

## Conflicts of interest

The authors declare no conflict of interest.

## Acknowledgements

This work was supported by the National Natural Science Foundation of China (31801784, 31572042), the Natural Science Foundation of Heilongjiang Province (ZD2017002), Heilongjiang Province Postdoctoral Science Foundation (LBH-Z16030), the Research Science Foundation in Technology Innovation of Harbin (2017RAQXJ017), the "Academic Backbone" Project of Northeast Agricultural University (16XG24), Heilongjiang Province Students' Innovation and Entrepreneurship Training Program (201810224067), and the Northeast Agricultural University Students' Innovation and Entrepreneurship Training Program (2019).

## References

- M. R. Blumhorst and J. B. Weber, *Pest Manage. Sci.*, 2010, **42**, 79–84.
- J. X. Li and X. S. Zhang, *J. Inclusion Phenom. Macrocyclic Chem.*, 2011, **69**, 173–179.
- V. Gupta, M. Davis, L. J. Hope-Weeks and F. Ahsan, *Pharm. Res.*, 2011, **28**, 1733.
- C. Schönbeck, R. Holm, P. Westh and G. H. Peters, *J. Inclusion Phenom. Macrocyclic Chem.*, 2014, **78**, 351–361.
- S. Gao, C. Bie, Y. Liu, T. Zhang, Y. Fu and F. Ye, *Polymers*, 2018, **10**, 1294.
- S. Wang, L. Kong, Y. Zhao, L. Tan, J. Zhang, Z. Du and H. Zhang, *Food Hydrocolloids*, 2019, **93**, 270–275.



- 7 A. Lodagekar, R. M. Borkar, S. Thatikonda, R. B. Chavan, V. Naidu, N. R. Shastri, R. Srinivas and N. Chella, *Carbohydr. Polym.*, 2019, **212**, 252–259.
- 8 M. Kfoury, C. Geagea, S. Ruellan, H. Greige-Gerges and S. Fourmentin, *Food Chem.*, 2019, **278**, 163–169.
- 9 S. W. Jun, M. S. Kim, J. S. Kim, H. J. Park, S. Lee, J. S. Woo and S. J. Hwang, *Eur. J. Pharm. Biopharm.*, 2007, **66**, 413–421.
- 10 R. Patel and N. Purohit, *AAPS PharmSciTech*, 2009, **10**, 1301–1312.
- 11 T. Higuchi, *Adv. Anal. Chem. Instrum.*, 1965, **4**, 117–212.
- 12 T. Loftsson, D. Hreinsdóttir and M. Másson, *Int. J. Pharm.*, 2005, **302**, 18–28.
- 13 J. Chao, H. Wang, W. Zhao, M. Zhang and L. Zhang, *Int. J. Biol. Macromol.*, 2012, **50**, 277–282.
- 14 C. Folch-Cano, M. Yazdani-Pedram and C. Olea-Azar, *Molecules*, 2014, **19**, 14066–14079.
- 15 Y. Fu, S. Q. Zhang, Y. X. Liu, J. Y. Wang, S. Gao, L. X. Zhao and F. Ye, *Ind. Crops Prod.*, 2019, **137**, 566–575.
- 16 F. Ye, Y. Zhai, T. Kang, S. L. Wu, J. J. Li, S. Gao, L. X. Zhao and Y. Fu, *Pestic. Biochem. Physiol.*, 2019, **157**, 60–68.
- 17 Y. Fu, K. Wang, P. Wang, J. X. Kang, S. Gao and F. Ye, *Front. Chem.*, 2019, **7**, 10.
- 18 Y. Fu, Y. X. Liu, K. H. Yi, M. Q. Li, J. Z. Li and F. Ye, *Front. Chem.*, 2019, **7**, 556.
- 19 C. Yáñez, P. Cañete-Rosales, J. P. Castillo, N. Catalán, T. Undabeytia and E. Morillo, *PLoS One*, 2012, **7**, e41072.
- 20 C. Yuan, Z. Lu and Z. Jin, *Food Chem.*, 2014, **152**, 140–145.
- 21 J. Zhang, B. Li, H. Bi and P. Zhang, *Trans. Tianjin Univ.*, 2014, **20**, 350–357.
- 22 X. Yan, Y. Shi, C. Qiao, Y. Li, X. Wei and X. Qiao, *Mater. Sci. Eng., C: Biomimetic Supramol. Syst.*, 2017, **78**, 1016–1022.
- 23 R. O. Williams, V. Mahaguna and M. Sriwongjanya, *Eur. J. Pharm. Biopharm.*, 1998, **46**, 355–360.
- 24 A. P. Mukne and M. J. A. P. Nagarsenker, *AAPS PharmSciTech*, 2004, **5**, 142.
- 25 A. Figueiras, L. Ribeiro, M. T. Vieira and F. Veiga, *J. Inclusion Phenom. Macrocyclic Chem.*, 2007, **57**, 173–177.
- 26 M. D. Antunes, G. da Silva Dannenberg, Á. M. Fiorentini, V. Z. Pinto, L.-T. Lim, E. da Rosa Zavareze and A. R. G. Dias, *Int. J. Biol. Macromol.*, 2017, **104**, 874–882.
- 27 P. Mura, E. Adragna, A. Rabasco, J. Moyano, J. Perez-Martinez, M. Arias and J. M. Gines, *Drug Dev. Ind. Pharm.*, 1999, **25**, 279–287.
- 28 S. Gao, Y. Liu, J. Jiang, Q. Ji, Y. Fu, L. Zhao, C. Li and F. Ye, *J. Mol. Liq.*, 2019, **293**, 111513, DOI: 10.1016/j.molliq.2019.111513.
- 29 F. Ye, P. Ma, Y. Y. Zhang, P. Li, F. Yang and Y. Fu, *Front. Plant Sci.*, 2018, **9**, 1850.

